VIP Heterolytic H_2 Cleavage | Very Important Paper

DOI: 10.1002/ange.201402090

Heterolytic Cleavage of Hydrogen by an Iron Hydrogenase Model: An Fe-H···H-N Dihydrogen Bond Characterized by Neutron Diffraction**

Tianbiao Liu, Xiaoping Wang, Christina Hoffmann, Daniel L. DuBois, and R. Morris Bullock**

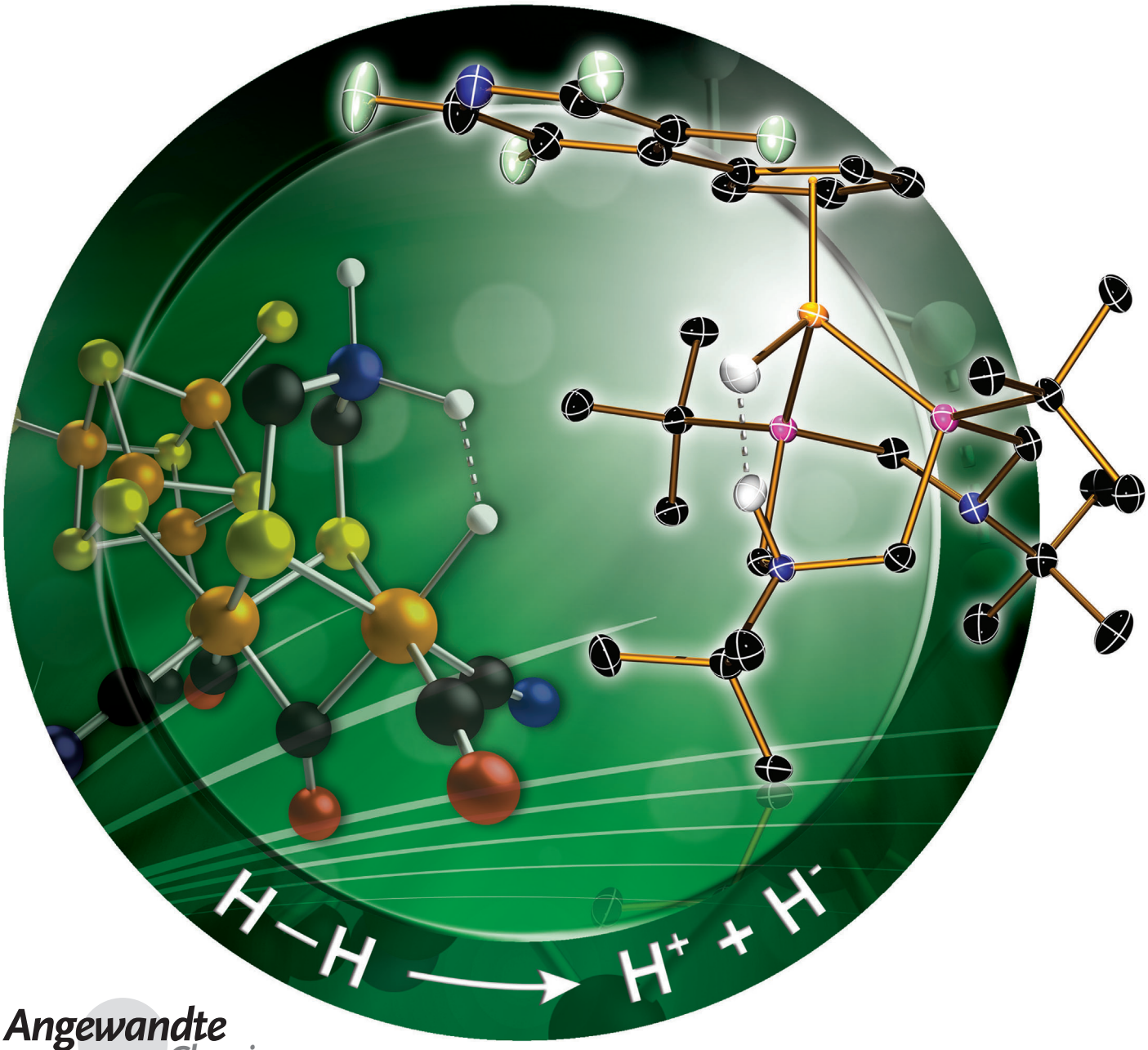

Abstract: *Hydrogenase enzymes in nature use hydrogen as a fuel, but the heterolytic cleavage of H–H bonds cannot be readily observed in enzymes. Here we show that an iron complex with pendant amines in the diphosphine ligand cleaves hydrogen heterolytically. The product has a strong Fe-H···H-N dihydrogen bond. The structure was determined by single-crystal neutron diffraction, and has a remarkably short H···H distance of 1.489(10) Å between the protic N-H$^{\delta+}$ and hydridic Fe-H$^{\delta-}$ part. The structural data for [Cp^{C_5F_4N}Fe**H**(P$^{tBu}_2$N$^{tBu}_2$**H**)]$^+$ provide a glimpse of how the H–H bond is oxidized or generated in hydrogenase enzymes. These results now provide a full picture for the first time, illustrating structures and reactivity of the dihydrogen complex and the product of the heterolytic cleavage of H_2 in a functional model of the active site of the [FeFe] hydrogenase enzyme.*

Use of hydrogen as a fuel by hydrogenase enzymes[1] in nature requires heterolytic cleavage of the H–H bond into a proton (H^+) and a hydride (H^-), a reaction that is also a critical step in homogeneous catalysts for the hydrogenation of C=O and C=N bonds.[2] Iron, which is earth-abundant and inexpensive,[3] is essential in the active site of both the [FeFe] hydrogenase and the [NiFe] hydrogenase, spurring intense efforts to model their reactivity with synthetic iron complexes.[4] An understanding of the catalytic oxidation of H_2 by hydrogenases provides insights into the design of synthetic catalysts that are sought as cost-effective alternatives to the use of the precious metal platinum in fuel cells.[4b,5] Crystallographic studies on the [FeFe] hydrogenase enzyme[6] were critical to understand its reactivity, but the key H–H bond cleavage step is not readily observed experimentally in natural hydrogenases. Limitations on the precise location of hydrogen atoms by X-ray diffraction can be overcome by use of neutron diffraction,[7] though its use is often limited by the difficulty of obtaining suitable crystals and by the scarcity of neutron sources. We herein report that an iron complex with a pendant amine in the diphosphine ligand cleaves hydrogen heterolytically under mild conditions, leading to [Cp^{C_5F_4N}FeH(P$^{tBu}_2$N$^{tBu}_2$H)]$^+$BAr$^F_4{}^-$ (Cp^{C_5F_4N} = tetrafluoropyridylcyclopentadienide; P$^{tBu}_2$N$^{tBu}_2$ = 1,5-di(*tert*-butyl)-3,7-di(*tert*-butyl)-1,5-diaza-3,7-diphosphacyclooctane; Ar^F = 3,5-bis(trifluoromethyl)phenyl; Scheme 1). The Fe-H···H-N moiety has a strong dihydrogen bond,[8] with a remarkably short H···H distance of 1.489(10) Å between the protic N-H$^{\delta+}$ and hydridic Fe-H$^{\delta-}$ part. The structural data for [Cp^{C_5F_4N}FeH(P$^{tBu}_2$N$^{tBu}_2$H)]$^+$ provide a glimpse of how the H–H bond is oxidized or generated in hydrogenase enzymes,[9] with the pendant amine playing a key role as a proton relay.

We previously reported that H_2/D_2 scrambling is catalyzed by [CpFe(P$^{Ph}_2$N$^{Bn}_2$)(H$_2$)]BAr$^F_4$ (Bn = benzyl), which mimics hydrogenase activity and implicates heterolytic cleavage of H_2 (and D_2) by [CpFe(P$^{Ph}_2$N$^{Bn}_2$)]BAr$^F_4$.[10] On the basis of single-crystal X-ray diffraction and solution NMR spectroscopic measurements, the H–H distance of the bound H_2 ligand of [CpFe(P$^{Ph}_2$N$^{Bn}_2$)(H$_2$)]$^+$ was found to be 0.94 Å. Modifying the ligands by adding an electron-withdrawing C_6F_5 group to the Cp ligand and changing from benzyl to *tert*-butyl groups on the phosphines led to [Cp^{C_6F_5}Fe(P$^{tBu}_2$N$^{Bn}_2$)H], which is an electrocatalyst for the oxidation of H_2.[11]

The iron complex [Cp^{C_5F_4N}Fe(P$^{tBu}_2$N$^{tBu}_2$)Cl] (**[1-Cl]**, Figure 1) was synthesized and fully characterized by ^{1}H, ^{31}P, and ^{19}F NMR spectroscopy. Addition of NaBAr$^F_4$ readily produces [Cp^{C_5F_4N}Fe(P$^{tBu}_2$N$^{tBu}_2$)]BAr$^F_4$ (**[1]BAr$^F_4$**) with a Lewis acidic Fe center and basic pendant amines in the diphosphine ligand. While this complex is drawn as having a vacant coordination site, the pendant amine may be weakly bound to the Fe, as found for a Mn complex[12] and a Cr complex[13] with a P_2N_2 ligand. Further studies to evaluate the bonding of **[1]BAr$^F_4$** will be reported.

Exposure of a dark brown solution of **[1]BAr$^F_4$** to H_2 (1 atm) immediately generates an orange solution (Scheme 1) of **[1-Fe*H*(N*H*)]BAr$^F_4$** that has a distinctly different color from the typical yellow color of similar [Fe(H$_2$)]$^+$ complexes.[10] The formation of **[1-Fe*H*(N*H*)]BAr$^F_4$** presumably proceeds through an unobserved [Fe(H$_2$)]$^+$ intermediate (**[1-Fe(H$_2$)]$^+$**) generated by the uptake of H_2 by **[1]BAr$^F_4$** (Scheme 1). The structure of **[1-Fe*H*(N*H*)]BAr$^F_4$** was determined by single-crystal neutron diffraction, and shows that heterolytic cleavage of H_2 occurred, with the hydride transferred to the iron core and the proton located on the pendant amine (Figure 1).[14] The Fe-H distance is 1.544(7) Å, and the N-H distance is 1.097(10) Å. The H···H bond distance of 1.489(10) Å is significantly longer than the H–H distance (0.94 Å) of [Cp^{C_6F_5}Fe(P$^{tBu}_2$N$^{Bn}_2$)(H$_2$)]BAr$^F_4$.[11] Although the covalent H–H bond was cleaved, the remarkably short H···H separation reveals a strong dihydrogen bond[8] between the protic NH$^{\delta+}$ and the hydridic FeH$^{\delta-}$.

Non-bonding H···H distances are typically greater than 2.4 Å, which is twice the van der Waals radius for H, though shorter distances have been found in some molecules with unusual geometries.[15] The H···H separation observed in **[1-Fe*H*(N*H*)]BAr$^F_4$** is the shortest found for any H···H distance that is not covalently bound, to the best of our knowledge. Several iridium complexes with dihydrogen bonds (Ir-H···H-

[*] Dr. T. Liu, Dr. D. L. DuBois, Dr. R. M. Bullock
Center for Molecular Electrocatalysis
Pacific Northwest National Laboratory
P.O. Box 999, Richland, WA 99352 (USA)
E-mail: Tianbiao.Liu@pnnl.gov
morris.bullock@pnnl.gov
Dr. X. Wang, Dr. C. Hoffmann
Chemical and Engineering Materials Division
Oak Ridge National Laboratory
Oak Ridge, TN 37831 (USA)

[**] This research was supported as part of the Center for Molecular Electrocatalysis, an Energy Frontier Research Center funded by the U.S. Department of Energy, Office of Science, Office of Basic Energy Sciences. Pacific Northwest National Laboratory is operated by Battelle for the U.S. Department of Energy. We thank Dr. Molly O'Hagan for assistance with HSQC NMR experiments and Dr. John A. S. Roberts for assistance with the electrochemical studies. Research conducted at ORNL's Spallation Neutron Source was sponsored by the Scientific User Facilities Division, Office of Basic Energy Sciences, U.S. Department of Energy. ORNL is managed by UT-Battelle, LLC, for the U.S. Department of Energy under contract No. DE-AC05-00OR22725.

Supporting information for this article is available on the WWW under http://dx.doi.org/10.1002/anie.201402090.

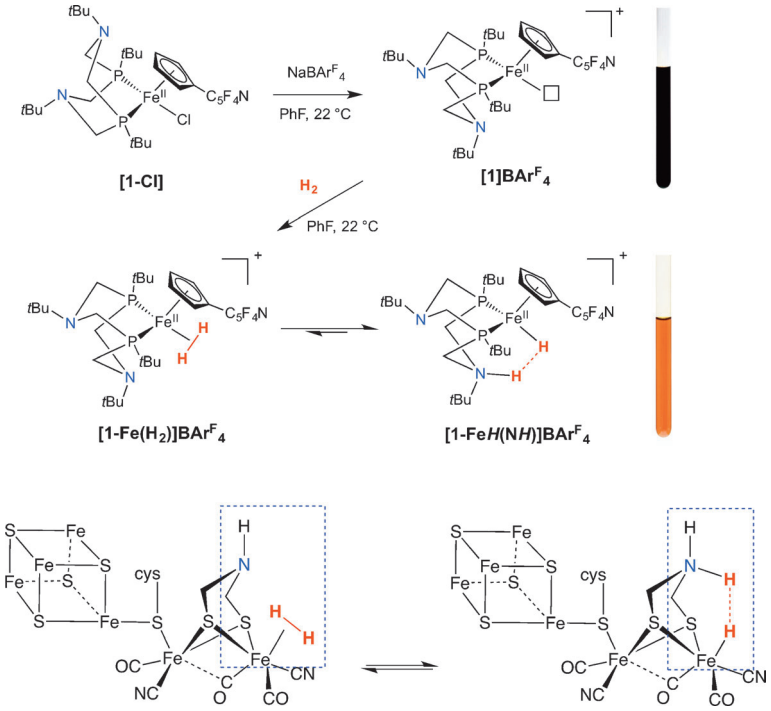

Scheme 1. Top: Synthesis of the 16-electron unsaturated Fe complex (open square indicates a vacant coordination site) and its reaction with H_2, leading to the heterolytic cleavage product. Photographs at the right side show NMR tubes containing **[1]**$^+$ and **[1-Fe*H*(N*H*)]**$^+$. Bottom: Analogous binding of H_2 and heterolytic cleavage of H_2 by the [FeFe] hydrogenase.

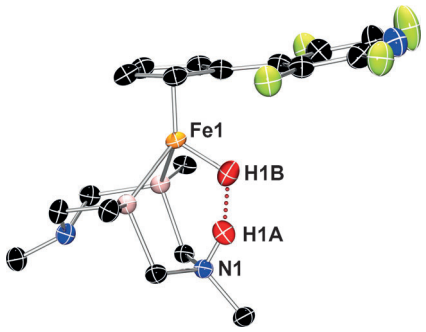

Figure 1. Molecular structure of **[1-Fe*H*(N*H*)]BAr$^F_4$** determined by neutron diffraction, showing thermal ellipsoids at 50% probability. For clarity, the methyl substituents of the P$^{tBu}_2$N$^{tBu}_2$ ligand, the BAr$^F_4{}^-$ anion, the co-crystallized fluorobenzene molecule, and hydrogen atoms bonded to carbon atoms are omitted. Selected distances (Å) and angles (°) for **[1-Fe*H*(N*H*)]**$^+$: H1A···H1B 1.489(10); Fe1–H1B 1.544(7); N1–H1A 1.079(6); H1B-H1A-N1 155.6(8); P1-Fe1-P2 83.62(11).

N) have been reported by Crabtree and co-workers[16] and by Morris and co-workers,[17] with the H···H separations estimated around 1.75–1.9 Å on the basis of X-ray diffraction and/or NMR spectroscopic measurements. An unusual intermolecular dihydrogen bond was characterized by neutron diffraction: the adduct formed between indole and [ReH$_5$(PPh$_3$)$_3$] exhibited an H···H separation of 1.734(8) Å.[18]

If the structure of **[1-Fe*H*(N*H*)]**$^+$ in solution were the same as that established in the solid state by neutron diffraction, then a resonance for Fe-H would be expected in the ^{1}H NMR spectrum with a chemical shift similar to the resonance at −16.0 ppm for [CpFe(P$^{Ph}_2$N$^{Bn}_2$)(H)].[10] Instead, a broad singlet integrating to two protons was observed at −5.30 ppm in CD_2Cl_2 at 22 °C and remained unchanged at −80 °C. A ^{15}N–^{1}H heteronuclear single-quantum coherence (HSQC) spectrum of **[1-Fe*H*(N*H*)]BAr$^F_4$** in CD_2Cl_2 at −70 °C exhibits a cross peak between the resonance of the pendant amine nitrogen atom (−293 ppm in the ^{15}N NMR spectrum) and the resonance at −5.36 ppm (Figure S3). These and other NMR spectroscopy experiments, including deuterium (^{2}H) labeling, are consistent with rapid intramolecular hydride–proton exchange of the Fe*H* and N*H* resonances. This dynamic behavior indicates extremely fast, reversible heterolytic formation and cleavage of the H–H bond through the intermediate **[1-Fe(H$_2$)]**$^+$, where the H–H bond is regenerated. Dynamic NMR studies lead to an estimated lower limit of the exchange rate of $2.2 \times 10^4\ s^{-1}$ at −80 °C, corresponding to a rate of approximately $2.2 \times 10^7\ s^{-1}$ at 22 °C (see the Supporting Information for details). A similar reversible heterolytic cleavage of H_2 was recently observed in a MnH/NH complex that also has pendant amines in the diphosphine ligand.[12]

DFT calculations show that **[1-Fe*H*(N*H*)]**$^+$ is approximately 0.65 kcal mol^{-1} more stable than **[1-Fe(H$_2$)]**$^+$ (Figure 2). The transition state for the heterolytic cleavage of H_2 was located, giving a reaction barrier of $\Delta G^{\ddagger} = 3.29$ kcal mol^{-1}, which is consistent with the estimated maximum value (< 7.3 kcal mol^{-1}, see the Supporting Information) from the NMR experiments. The low calculated barrier suggests that the rate of reversible heterolytic cleavage may be much higher than the estimated lower limit from the NMR experiments. The H–H distance calculated for **[1-Fe(H$_2$)]**$^+$ is 0.87 Å; it elongates to 0.95 Å in the transition state, and is calculated as 1.37 Å in **[1-Fe*H*(N*H*)]**$^+$. A natural bonding orbital (NBO) analysis gives a Wiberg bond index of 0.1 between the hydride and the proton, suggesting a substantial

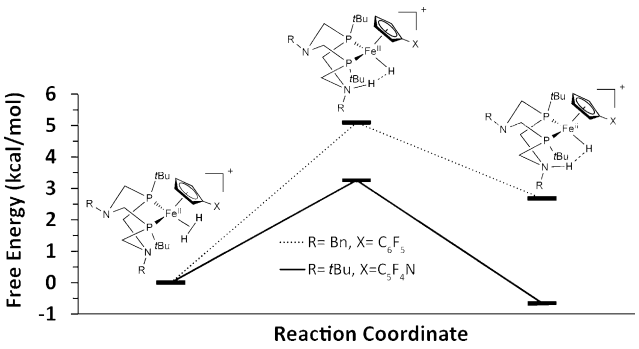

Figure 2. Computed lowest free energy pathway of H_2 cleavage by **[1-Fe(H$_2$)]**$^+$ (solid line) and **[Cp^{C_6H_5}Fe(P$^{tBu}_2$N$^{Bn}_2$)(H$_2$)]**$^+$ (dotted line).

dihydrogen bonding interaction. The calculated energy of $[Cp^{C_6F_5}Fe(P^{tBu}{}_2N^{Bn}{}_2)(H_2)]^+$ is 2.63 kcal mol^{-1} more stable than the Fe*H*N*H* tautomer $[Cp^{C_6F_5}Fe(P^{tBu}{}_2N^{Bn}{}_2H)(H)]$ (Figure 2), with an activation barrier of 5.09 kcal mol^{-1} for the H–H bond cleavage $[Cp^{C_6F_5}Fe(P^{tBu}{}_2N^{Bn}{}_2)(H_2)]^+$. The calculated barrier is consistent with our experimental observation of the $[Fe(H_2)]^+$ tautomer.[10] Our experimental and computational studies clearly show that carefully controlled changes in the electronic properties of the ligand shifts the thermodynamics of these Fe complexes to favor either H–H retention or heterolytic cleavage.

[1-Fe*H*(N*H*)]BAr$^F_4$ is an electrocatalyst for oxidation of H_2, so it serves as a functional model for the catalytic activity of [FeFe] hydrogenase enzymes. The cyclic voltammogram of **[1-Cl]** exhibits a reversible one-electron oxidation wave corresponding to the Fe^{III}/Fe^{II} couple at −0.54 V versus the $Cp_2Fe^{+/0}$ couple (Figure 3, red trace). **[1-Fe*H*(N*H*)]BAr$^F_4$** exhibits quasi-reversible redox waves at 0.29 V ($Fe^{III/II}$ couple) and −1.53 V ($Fe^{II/I}$ couple; Figure 3, blue trace).

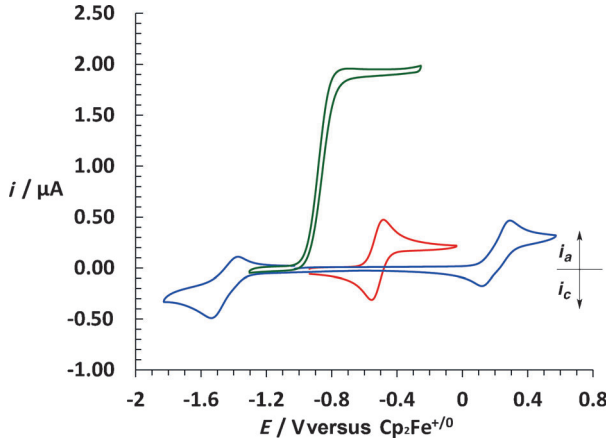

Figure 3. Cyclic voltammograms that indicate catalytic oxidation of H_2 (1.0 atm) using **[1-Fe*H*(N*H*)]BAr$^F_4$** (1.0 mM) in the presence of *N*-methylpyrrolidine (60 mM). The red trace is a cyclic voltammogram of **[1-Cl]** (1.0 mM). The blue trace is a cyclic voltammogram of **[1-Fe*H*(N*H*)]BAr$^F_4$** (1.0 mM) generated in situ from **[1-Cl]** by adding 1.0 equiv $NaBAr^F_4$ under 1.0 atm H_2. The green trace is a cyclic voltammogram recorded after adding 60 equiv *N*-methylpyrrolidine (60 mM). Conditions: scan rate 20 mV s^{-1}, PhF as solvent, 0.1 M $nBu_4NB(C_6F_5)_4$ as supporting electrolyte; glassy carbon working electrode. Potentials are referenced to $Cp_2Fe^{+/0}$.

The addition of an excess amount of base (*N*-methylpyrrolidine) to a solution of **[1-Fe*H*(N*H*)]BAr$^F_4$** led to the catalytic oxidation of H_2, as indicated by the plateau shape observed at a half-wave potential of −0.86 V (Figure 3, green trace). The turnover frequency for the oxidation of H_2 was determined to be 0.9 s^{-1}. The overpotential at the half-wave potential was determined to be 95 mV (see the Supporting Information for the determination of the rate constant and overpotential). The proposed mechanism is analogous to that proposed for $[Cp^{C_6F_5}Fe(P^{tBu}{}_2N^{Bn}{}_2)H]$.[11]

These results provide a full picture of the structures and reactivity of the $[Fe(H_2)]^+$ complex and the product of the heterolytic cleavage of H_2 in a functional model of the active site of the [FeFe] hydrogenase enzyme. DFT calculations by Fan and Hall on a structural model of the [FeFe] hydrogenase provided theoretical evidence for a $[Fe(H_2)]$ species and subsequent intramolecular H–H bond cleavage.[19] The resultant Fe-H···H-N species had a dihydrogen bond with a computed H···H distance of 1.472 Å, which is nearly identical to the H···H distance we found in **[1-Fe*H*(N*H*)]$^+$**. However, the $Fe(H_2)$ and Fe-H···H-N states of the active site of hydrogenase have never been experimentally observed. Rauchfuss and co-workers recently reported[20] a structural study of a model of the [FeFe] hydrogenase active site $([(H)Fe_2(S_2NH)(CO)_2(dppv)_2]^{2+}$, where S_2NH is the protonated azadithiolate ligand $[(SCH_2)_2NH_2]^-$ and dppv is *cis*-$C_2H_2(PPh_2)_2$) featuring a dihydrogen bond between a terminal iron hydride and the NH proton. In that complex, the H···H distance was determined by X-ray diffraction as 1.88(7) Å. The dihydrogen bond of $[(H)Fe_2(S_2NH)(CO)_2(dppv)_2]^{2+}$ was formed by protonation of the azadithiolate ligand of the precursor, $[(H)Fe_2(S_2N)(CO)_2(dppv)_2]^+$, rather than by heterolytic cleavage of H_2; observation of the corresponding dihydrogen complex $[(H_2)Fe_2(S_2N)(CO)_2(dppv)_2]^{2+}$ has not been reported.

Our results provide experimental support for the previously proposed binding of H_2 to the distal Fe in the ferrous oxidation state (dashed blue rectangle in Scheme 1) of the [FeFe] hydrogenase enzyme and the participation of a pendant amine in the heterolytic cleavage of the bound dihydrogen molecule. The product of heterolytic cleavage has a strong Fe-H···H-N dihydrogen bond.

Experimental Section

The synthesis of $NaCp^{C_5F_4N}$, $P^{tBu}{}_2N^{tBu}{}_2$ $[Fe(P^{tBu}{}_2N^{tBu}{}_2)Cl_2]$, $[Cp^{C_5F_4N}Fe(P^{tBu}{}_2N^{tBu}{}_2)Cl]$, and $[Cp^{C_5F_4N}Fe(P^{tBu}{}_2N^{tBu}{}_2)]BAr^F_4$, experimental details of single-crystal X-ray diffraction and electrochemical H_2 oxidation, and DFT calculations are given in the Supporting Information.

$[Cp^{C_5F_4N}Fe(P^{tBu}{}_2N^{tBu}NH)(H)]BAr^F_4$, **[1-Fe*H*(N*H*)]BAr$^F_4$: [1-Cl]** (0.135 g, 0.200 mmol) and $NaBAr^F_4$ (0.190 g, 0.210 mmol) were dissolved in fluorobenzene (5 mL). Then H_2 gas (1.0 atm) was purged through the solution, resulting in a rapid color change from dark to orange, indicating the formation of **[1-Fe*H*(N*H*)]BAr$^F_4$**, which was confirmed by ^{1}H NMR and ^{31}P{^{1}H} NMR spectroscopy. After filtration to remove insoluble solids, **[1-Fe*H*(N*H*)]BAr$^F_4$** was precipitated by adding pentane (60 mL) to the filtrate. The resulting solid was collected by filtration and dried under vacuum for 30 min. The isolated **[1-Fe*H*(N*H*)]BAr$^F_4$** (0.254 g, yield, 82%) was stored under H_2 in a glovebox. Alternatively, **[1-Fe*H*(N*H*)]BAr$^F_4$** can be prepared from **[1]BAr$^F_4$** and H_2. Elemental analysis (%) calcd for **[1-Fe*H*(N*H*)]BAr$^F_4$** ($C_{62}H_{58}BN_3F_{28}FeP_2$): C, 49.46; H, 3.88; N, 2.79. Found: C, 49.73; H, 4.13; N, 2.59. ^{1}H NMR ([D$_5$]PhCl, 22 °C): $\delta = 7.99$ (s, 8 H, $B(C_8F_6H_3)_4$), 7.38 (s, 4 H, $B(C_8F_6H_3)_4$), 4.82 (s, 2 H, $C_6F_5C_5H_4$), 4.26 (s, 2 H, $C_6F_5C_5H_4$), 3.00 (s, 2 H, $NCH_2C_6H_5$), 2.05 (d, $J_{HH} = 10.0$ Hz, 2 H, $NCH_2C_6H_5$), 1.98 (s, 2 H, NCH_2P), 1.86 (d, $J_{HH} = 10.0$ Hz, 2 H, NCH_2P), 0.76 (t, $J_{PH} = 10.0$ Hz, 18 H, $PC(CH_3)_3$), 0.62 (s, 9 H, $NC(CH_3)_3$), 0.59 (s, 9 H, $NC(CH_3)_3$), −7.06 ppm (s, br, 2 H, the averaged signal of Fe*H* and N*H*). In CD_2Cl_2 at 22 °C and at −80 °C, the averaged resonance of Fe*H* and N*H* appears at −5.36 ppm. ^{31}P{^{1}H} NMR ([D$_5$]PhCl): $\delta = 91.3$ ppm. ^{19}F NMR ([D$_5$]PhCl): $\delta = -87.7$ (m, 2 F, C_5F_4N), −137.3 ppm (m, 2 F, C_5F_4N). ^{15}N–^{1}H HSQC (heteronuclear single-quantum correlation spectroscopy, CD_2Cl_2, −70 °C): a cross peak was observed between the proton resonance at −5.30 ppm (the averaged signal of Fe*H* and N*H*) and the nitrogen resonance at −294 ppm (*N*H) (see Figure S3).

Neutron diffraction studies: The single-crystal neutron diffraction experiment was performed using the TOPAZ single-crystal time-of-flight Laue diffractometer at the Spallation Neutron Source, Oak Ridge National Laboratory.[21] Details are provided in the Supporting Information.

Received: February 4, 2014
Published online: April 22, 2014

Keywords: enzyme models · hydrogen · hydrogenases · iron · neutron diffraction

[1] a) J. A. Cracknell, K. A. Vincent, F. A. Armstrong, *Chem. Rev.* **2008**, *108*, 2439 – 2461; b) C. Tard, C. J. Pickett, *Chem. Rev.* **2009**, *109*, 2245 – 2274; c) J. C. Fontecilla-Camps, A. Volbeda, C. Cavazza, Y. Nicolet, *Chem. Rev.* **2007**, *107*, 4273 – 4303.

[2] a) R. Noyori, *Angew. Chem.* **2002**, *114*, 2108 – 2123; *Angew. Chem. Int. Ed.* **2002**, *41*, 2008 – 2022; b) A. A. Mikhailine, M. I. Maishan, A. J. Lough, R. H. Morris, *J. Am. Chem. Soc.* **2012**, *134*, 12266 – 12280; c) W. Zuo, A. J. Lough, Y. Li, R. H. Morris, *Science* **2013**, *342*, 1080 – 1083.

[3] a) *Catalysis Without Precious Metals* (Ed.: R. M. Bullock), Wiley-VCH, Weinheim, **2010**; b) R. M. Bullock, *Science* **2013**, *342*, 1054 – 1055.

[4] a) S. Ogo, K. Ichikawa, T. Kishima, T. Matsumoto, H. Nakai, K. Kusaka, T. Ohhara, *Science* **2013**, *339*, 682 – 684; b) T. R. Simmons, V. Artero, *Angew. Chem.* **2013**, *125*, 6259 – 6261; *Angew. Chem. Int. Ed.* **2013**, *52*, 6143 – 6145.

[5] a) M. Hambourger, M. Gervaldo, D. Svedruzic, P. W. King, D. Gust, M. Ghirardi, A. L. Moore, T. A. Moore, *J. Am. Chem. Soc.* **2008**, *130*, 2015 – 2022; b) S. Krishnan, F. A. Armstrong, *Chem. Sci.* **2012**, *3*, 1015 – 1023; c) F. Gloaguen, T. B. Rauchfuss, *Chem. Soc. Rev.* **2009**, *38*, 100 – 108; d) M. L. Singleton, N. Bhuvanesh, J. H. Reibenspies, M. Y. Darensbourg, *Angew. Chem.* **2008**, *120*, 9634 – 9637; *Angew. Chem. Int. Ed.* **2008**, *47*, 9492 – 9495.

[6] a) J. W. Peters, W. N. Lanzilotta, B. J. Lemon, L. C. Seefeldt, *Science* **1998**, *282*, 1853 – 1858; b) Y. Nicolet, C. Piras, P. Legrand, C. E. Hatchikian, J. C. Fontecilla-Camps, *Structure* **1999**, *7*, 13 – 23.

[7] R. Bau, R. G. Teller, S. W. Kirtley, T. F. Koetzle, *Acc. Chem. Res.* **1979**, *12*, 176 – 183.

[8] a) T. Richardson, S. de Gala, R. H. Crabtree, P. E. M. Siegbahn, *J. Am. Chem. Soc.* **1995**, *117*, 12875 – 12876; b) R. Custelcean, J. E. Jackson, *Chem. Rev.* **2001**, *101*, 1963 – 1980.

[9] a) G. Berggren, A. Adamska, C. Lambertz, T. R. Simmons, J. Esselborn, M. Atta, S. Gambarelli, J. M. Mouesca, E. Reijerse, W. Lubitz, T. Happe, V. Artero, M. Fontecave, *Nature* **2013**, *499*, 66 – 69; b) A. Silakov, B. Wenk, E. Reijerse, W. Lubitz, *Phys. Chem. Chem. Phys.* **2009**, *11*, 6592 – 6599; c) J. Esselborn, C. Lambertz, A. Adamska-Venkatesh, T. Simmons, G. Berggren, J. Noth, J. Siebel, A. Hemschemeier, V. Artero, E. Reijerse, M. Fontecave, W. Lubitz, T. Happe, *Nat. Chem. Biol.* **2013**, *9*, 607 – 609.

[10] T. Liu, S. Chen, M. J. O'Hagan, M. Rakowski DuBois, R. M. Bullock, D. L. DuBois, *J. Am. Chem. Soc.* **2012**, *134*, 6257 – 6272.

[11] T. Liu, D. L. DuBois, R. M. Bullock, *Nat. Chem.* **2013**, *5*, 228 – 233.

[12] E. B. Hulley, K. D. Welch, A. M. Appel, D. L. DuBois, R. M. Bullock, *J. Am. Chem. Soc.* **2013**, *135*, 11736 – 11739.

[13] M. T. Mock, S. Chen, R. Rousseau, M. J. O'Hagan, W. G. Dougherty, W. S. Kassel, D. L. DuBois, R. M. Bullock, *Chem. Commun.* **2011**, *47*, 12212 – 12214.

[14] CCDC 984485 (X-ray diffraction), 984486 (neutron diffraction) contain the supplementary crystallographic data for this paper. These data can be obtained free of charge from The Cambridge Crystallographic Data Centre via www.ccdc.cam.ac.uk/data_request/cif.

[15] J. Zong, J. T. Mague, R. A. Pascal, Jr., *J. Am. Chem. Soc.* **2013**, *135*, 13235 – 13237.

[16] a) R. H. Crabtree, P. E. M. Siegbahn, O. Eisenstein, A. L. Rheingold, T. F. Koetzle, *Acc. Chem. Res.* **1996**, *29*, 348 – 354; b) E. Peris, J. C. Lee, Jr., J. R. Rambo, O. Eisenstein, R. H. Crabtree, *J. Am. Chem. Soc.* **1995**, *117*, 3485 – 3491; c) J. C. Lee, Jr., E. Peris, A. L. Rheingold, R. H. Crabtree, *J. Am. Chem. Soc.* **1994**, *116*, 11014 – 11019.

[17] A. J. Lough, S. Park, R. Ramachandran, R. H. Morris, *J. Am. Chem. Soc.* **1994**, *116*, 8356 – 8357.

[18] J. Wessel, J. C. Lee, Jr., E. Peris, G. P. A. Yap, J. B. Fortin, J. S. Ricci, G. Sini, A. Albinati, T. F. Koetzle, O. Eisenstein, A. L. Rheingold, R. H. Crabtree, *Angew. Chem.* **1995**, *107*, 2711 – 2713; *Angew. Chem. Int. Ed. Engl.* **1995**, *34*, 2507 – 2509.

[19] H.-J. Fan, M. B. Hall, *J. Am. Chem. Soc.* **2001**, *123*, 3828 – 3829.

[20] M. E. Carroll, B. E. Barton, T. B. Rauchfuss, P. J. Carroll, *J. Am. Chem. Soc.* **2012**, *134*, 18843 – 18852.

[21] G. Jogl, X. Wang, S. A. Mason, A. Kovalevsky, M. Mustyakimov, Z. Fisher, C. Hoffman, C. Kratky, P. Langan, *Acta Crystallogr. Sect. D* **2011**, *67*, 584 – 591.